

Forward inclusive dijet production and azimuthal correlations in pA collisions

Cyrille Marquet*

RIKEN BNL Research Center, Brookhaven National Laboratory, Upton, NY 11973, USA

We derive forward inclusive dijet production in the scattering of a dilute hadron off an arbitrary dense target, whose partons with small fraction of momentum x are described by a Color Glass Condensate. Both multiple scattering and non-linear QCD evolution at small- x are included. This is of relevance for measurements of two-particle correlations in the proton direction of proton-nucleus collisions at RHIC and LHC energies. The azimuthal angle distribution is peaked back to back and broadens as the momenta of the measured particles gets closer to the saturation scale.

I. INTRODUCTION

Understanding particle correlations in nucleus-nucleus collisions has been the purpose of many studies in recent years at the Relativistic Heavy Ion Collider (RHIC). These measurements provide insight on the properties of dense QCD matter, in particular they could help distinguish to what extent the experimental observations are due to initial-state or final-state effects. For instance, parton saturation [1] is a characteristic of the initial nuclear wave functions, and is usually entangled with the final-state phenomenon of medium-induced energy loss [2]. It is so in the suppression of high- p_T forward hadronic yields. By contrast, with measurements of particle correlations, initial-state and final-state effects may be disentangled.

As a complement to single inclusive particle spectra, or to nuclear modification factors, the simplest observables are obtained with two-particle correlations. In particular, the correlation in azimuthal angle can provide further insight on the dynamics of energy loss. For instance it has been argued [3] that the energy radiated off a hard final-state parton is expected to propagate in such a way that it should lead to an azimuthal correlation featuring a double-peak structure, instead of the standard back-to-back peak. This has been observed in Au-Au collisions, the away-side azimuthal correlation splits into a double peak with maxima displaced away from 180° . Meanwhile, the contribution of initial state saturation effects to the azimuthal decorrelation has yet to be determined.

The main purpose of the present work is to study the inclusive two-particle spectrum for the following process: $h\mathcal{T} \rightarrow h_1 h_2 X$ where h is a dilute hadron and the measured particles h_1 and h_2 are detected in the very forward direction of that hadron. In this case, only the high-momentum valence partons of h contribute to the scattering and the dominant partonic subprocess is $q\mathcal{T} \rightarrow qgX$: a valence quark emits a virtual gluon g via lowest-order pQCD Bremsstrahlung and the quark-gluon fluctuation is put on shell by the interaction with the target \mathcal{T} . In practice, this is relevant for forward particle production in deuteron-gold (d -Au) collisions at RHIC energies, where only valence quark contribute. For proton-lead (p -Pb) collisions at the LHC, even in the forward region, it is likely that one also needs to account for the $g \rightarrow q\bar{q}$ and $g \rightarrow gg$ subprocesses.

Meanwhile, it is suited to describe the target \mathcal{T} by a Color Glass Condensate (CGC), as the process is mainly probing partons with a very small fraction of momentum x : the energetic probes formed by the projectile's valence quark, and quark-gluon fluctuation, interact coherently over the whole longitudinal extension of the target, and see the small- x gluons inside \mathcal{T} as a dense system of weakly interacting gluons, that behave collectively. It has recently become clear, and it is manifest in the process of interest here, that the CGC cannot be described in terms of a single gluon distribution function, but rather must be described by n-point functions of Wilson-line operators. In other words, the so-called k_T -factorization used in [4] is not applicable. We explicitly derive the two-particle spectrum and obtain that it involves up to a 6-point function of Wilson lines in the fundamental representation. In addition, we do not restraint the calculation to the soft-gluon approximation as done in [5].

We obtain a formula similar to that of [6], but their counterpart of our n-point functions are treated differently than in the present paper. In this work, both multiple scattering and non-linear QCD evolution at small- x are included: the Wilson-line correlators are computed in the framework of the Balitsky-Kovchegov (BK) equation [7]. Considering the correlations in azimuthal angle, we obtain that the perturbative back-to-back peak of the azimuthal angle distribution, which we recover for very large momenta of the measured particles, is reduced by initial state saturation effects. As the momenta decrease closer to the saturation scale Q_s , the angular distribution broadens, but at RHIC and even LHC energies, saturation does not lead to a complete disappearance of the back-to-back peak.

*Electronic address: marquet@quark.phy.bnl.gov

The plan of the paper is as follows. In Section II, the inclusive two-particle spectrum $q\mathcal{T} \rightarrow qgX$ is calculated. The cross-section, differential with respect to the quark and gluon transverse momenta and rapidities, is expressed in terms of Wilson-line correlators in the CGC wavefunction. Section III is devoted to those CGC averages and describes how to perform them in the context of the BK evolution. In Section IV, we introduce the relevant observable to study the azimuthal angle correlation and we investigate the impact of the small- x evolution at RHIC and LHC energies.

II. FORWARD INCLUSIVE DIJET PRODUCTION CROSS-SECTION

In this section we derive the inclusive quark-gluon production cross-section in the high-energy scattering of a quark off a Color Glass Condensate. We shall work at leading order with respect to the strong coupling constant α_S , and to all orders with respect to $g_S \mathcal{A}$ where \mathcal{A} is the CGC color field. The relevant diagrams are shown in Fig.1 and the necessity of both diagrams will become transparent in the following derivation: it is a manifestation that there should be no gluon production without interaction with the target. We will later require that the scattering process features a hard momentum transfer $\Delta \gg \Lambda_{QCD}$, which justifies the use of perturbation theory.

We shall use light-cone coordinates with the incoming quark moving along the x^+ direction, and work in the light-cone gauge $\mathcal{A}^+ = 0$. In this case, when the quark passes through the CGC and interacts with its color field, the dominant couplings are eikonal: the partonic components of the dressed quark wavefunction have frozen transverse coordinates and the gluonic field of the target does not vary during the interaction. This is justified since the incident projectile propagates at nearly the speed of light and its time of propagation through the target is shorter than the natural time scale on which the target fields vary. The effect of the interaction with the target is that the components of the dressed quark wavefunction pick up eikonal phases.

A. The dressed quark wavefunction

To describe the wavefunction of the incoming quark, we shall use light-cone perturbation theory. We denote the 3-momentum of the quark $p = (p^+, p_\perp)$, and its spin and color indices α and i . One has $p^- = (p_\perp^2 + m^2)/2p^+$. To decompose its wavefunction on bare quark and gluon states, we introduce $b_{i,\alpha}^\dagger(k)$ and $b_{i,\alpha}(k)$ (resp. $a_{c,\lambda}^\dagger(k)$ and $a_{c,\lambda}(k)$), the creation and annihilation operators of a quark with color i , spin α (resp. gluon with color c , polarization λ), and 3-momentum k . One has

$$b_{i,\alpha}^\dagger(k)|0\rangle = |k, i, \alpha\rangle_0, \quad b_{i,\alpha}(k)|0\rangle = 0, \quad \{b_{i,\alpha}(k), b_{j,\beta}^\dagger(k')\} = \delta_{ij}\delta_{\alpha\beta}\delta^{(3)}(k - k'), \quad (1)$$

$$a_{c,\lambda}^\dagger(k)|0\rangle = |k, c, \lambda\rangle_0, \quad a_{c,\lambda}(k)|0\rangle = 0, \quad [a_{c,\lambda}(k), a_{d,\lambda'}^\dagger(k')] = \delta_{cd}\delta_{\lambda\lambda'}\delta^{(3)}(k - k'). \quad (2)$$

We recall that in light-cone quantization, the virtuality of the particle comes from the non-conservation of the momentum in the x^- direction, meaning $(k-k')^- \neq k^- - k'^-$. All particles are on-shell and only the 3-momentum is conserved.

We work at lowest order with respect to α_S so we only need to consider the Fock states $|q\rangle_0$ and $|qg\rangle_0$ in the decomposition of the dressed quark:

$$|p, i, \alpha\rangle = Z|p, i, \alpha\rangle_0 + \sum_{j\beta c\lambda} \int d^3k g_S T_{ij}^c \psi_{\alpha\beta}^\lambda(p, k) |(p-k, j, \beta); (k, c, \lambda)\rangle_0. \quad (3)$$

The $|qg\rangle_0$ part of the dressed quark is characterized by the wavefunction $g_S T_{ij}^c \psi_{\alpha\beta}^\lambda$ where β and j denote the spin and color indices of the quark and λ and c denote the polarization and color indices of the gluon. T^c is the generator of the fundamental representation of $SU(N_c)$ and $\psi_{\alpha\beta}^\lambda$ is given by

$$\psi_{\alpha\beta}^\lambda(p, k) = \frac{1}{\sqrt{8(p-k)^+ p^+ k^+}} \frac{\bar{u}_\beta(p-k) \gamma_\mu \varepsilon_{(\lambda)}^\mu(k) u_\alpha(p)}{(p-k)^- + k^- - p^-} \quad (4)$$

where $k = (k^+, k_\perp)$ and $p-k = (p^+ - k^+, p_\perp - k_\perp)$ are the 3-momenta of the gluon and quark respectively. The factor Z is a renormalization constant determined from the requirement that the normalization of the dressed quark is the same than that of the bare quark (note that those normalizations are proportional to $\delta^{(3)}(0)$ because we are using plane waves). Physically, Z accounts for the virtual gluon emission associated with the real gluon emission explicit in (3). When calculating inelastic processes, as is the case here, the actual value of Z is not relevant.

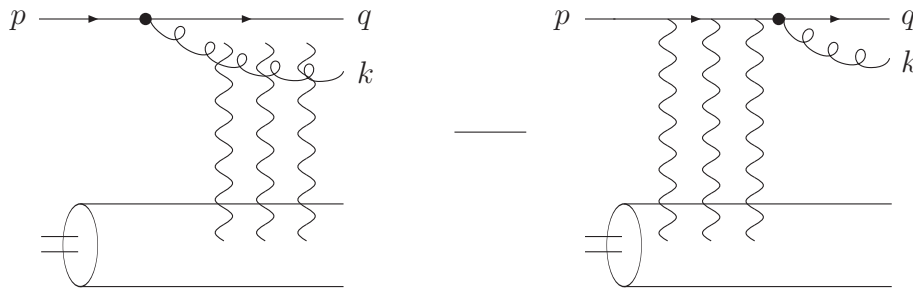


FIG. 1: Inclusive quark-gluon production cross-section in the high-energy scattering of a quark off a Color Glass Condensate. $p = (p^+, p_\perp)$: momentum of the incoming quark; $q = (q^+, q_\perp)$ and $k = (k^+, k_\perp)$: momentum of the outgoing quark and gluon. The vertical wavy lines represent the interaction with the target CGC, each line carries a factor $g_S \mathcal{A}$ and multiple gluon exchanges must be resummed. The black points represent the emission of the produced gluon by the quark, it is emitted before the interaction or after the interaction in which case the contribution comes with a minus sign, as explained in the text.

With our choice of gauge, one can write the two gluon polarization vectors $\varepsilon_{(1)}^\mu(k)$ and $\varepsilon_{(2)}^\mu(k)$ in terms of two transverse vectors ε_\perp^1 and ε_\perp^2 : $\varepsilon_{(\lambda)}^\mu(k) = (0, \varepsilon_\perp^\lambda, k_\perp \cdot \varepsilon_\perp^\lambda / k^+)$. Then using the chiral representation of the Dirac matrices to obtain the spinors leads to

$$\psi_{\alpha\beta}^\lambda(p, k) = \frac{1}{\sqrt{k^+}} \frac{1}{(k_\perp - zp_\perp)^2 + m^2 z^2} \begin{cases} \sqrt{2}(k_\perp - zp_\perp) \cdot \varepsilon_\perp^1 [\delta_{\alpha-}\delta_{\beta-} + (1-z)\delta_{\alpha+}\delta_{\beta+}] + mz^2 \delta_{\alpha+}\delta_{\beta-} & \lambda = 1 \\ \sqrt{2}(k_\perp - zp_\perp) \cdot \varepsilon_\perp^2 [\delta_{\alpha+}\delta_{\beta+} + (1-z)\delta_{\alpha-}\delta_{\beta-}] - mz^2 \delta_{\alpha-}\delta_{\beta+} & \lambda = 2 \end{cases} \quad (5)$$

with $z = k^+/p^+$. For reasons which will become clear later on, it is more convenient to work in a mixed space, in which the transverse momenta are Fourier transformed into transverse coordinates:

$$b_{i,\alpha}^\dagger(p^+, \mathbf{b}) = \int d^2b e^{-ip_\perp \cdot \mathbf{b}} b_{i,\alpha}^\dagger(p^+, p_\perp), \quad a_{c,\lambda}^\dagger(p^+, \mathbf{x}) = \int d^2b e^{-ip_\perp \cdot \mathbf{x}} a_{c,\lambda}^\dagger(p^+, p_\perp). \quad (6)$$

In the mixed representation, the decomposition of the dressed quark (3) on the Fock states $|q\rangle_0$ and $|qq\rangle_0$ is the following:

$$|p, i, \alpha\rangle = \int \frac{d^2b}{(2\pi)^2} e^{ip_\perp \cdot \mathbf{b}} \left[Z |p^+, \mathbf{b}, i, \alpha\rangle_0 + \sum_{j\beta c\lambda} \int dk^+ \frac{d^2x}{(2\pi)^2} g_S T_{ij}^c \phi_{\alpha\beta}^\lambda(p, k^+, \mathbf{x} - \mathbf{b}) |(p^+ - k^+, \mathbf{b}, j, \beta); (k^+, \mathbf{x}, c, \lambda)\rangle_0 \right] \quad (7)$$

where \mathbf{b} and \mathbf{x} are the transverse positions of the quark and gluon respectively, and with the mixed-space wavefunction

$$\phi_{\alpha\beta}^\lambda(p, k^+, \mathbf{x}) = \int d^2k_\perp e^{ik_\perp \cdot \mathbf{x}} \psi_{\alpha\beta}^\lambda(p, k) \quad (8)$$

given by

$$\phi_{\alpha\beta}^\lambda(p, k^+, \mathbf{x}) = \frac{2\pi m}{\sqrt{k^+}} e^{izp_\perp \cdot \mathbf{x}} \begin{cases} iz\sqrt{2}K_1(mz|\mathbf{x}|) \frac{\mathbf{x} \cdot \varepsilon_\perp^1}{|\mathbf{x}|} [\delta_{\alpha-}\delta_{\beta-} + (1-z)\delta_{\alpha+}\delta_{\beta+}] + z^2 K_0(mz|\mathbf{x}|) \delta_{\alpha+}\delta_{\beta-} & \lambda = 1 \\ iz\sqrt{2}K_1(mz|\mathbf{x}|) \frac{\mathbf{x} \cdot \varepsilon_\perp^2}{|\mathbf{x}|} [\delta_{\alpha+}\delta_{\beta+} + (1-z)\delta_{\alpha-}\delta_{\beta-}] - z^2 K_0(mz|\mathbf{x}|) \delta_{\alpha-}\delta_{\beta+} & \lambda = 2 \end{cases} \quad (9)$$

B. High-energy eikonal scattering off the target

Let us first recall the basics of the CGC description. When probing inside a target hadron with processes that are sensitive to partons with a very small fraction of momentum x , the probe actually sees a dense system of gluons, responsible for large classical color fields $\mathcal{A} \sim 1/g_S$ [8]. Rather than using a Fock-state decomposition which is not adapted to account for the collective behavior of the small- x gluons, it is more appropriate to use other degrees of freedom and describe the target by classical color fields:

$$|\mathcal{T}\rangle = |qqq\rangle_0 + |qqqg\rangle_0 + \dots + |qqqg \dots ggg\rangle_0 + \dots \quad \Rightarrow \quad |\mathcal{T}\rangle = \int D\mathcal{A} \Phi_{x_A}[\mathcal{A}] |\mathcal{A}\rangle. \quad (10)$$

The CGC wavefunction $\Phi_{x_A}[\mathcal{A}]$ is normalized such that $\int D\mathcal{A} |\Phi_{x_A}[\mathcal{A}]|^2 = 1$, and x_A denotes the smallest fraction of longitudinal momentum probed. It depends on the final-state kinematics of the process considered and will be specified later. The CGC wavefunction is mainly a non-perturbative quantity, but the x_A evolution of $|\Phi_{x_A}[\mathcal{A}]|^2$ can be computed from perturbative QCD [9], in the leading- $\ln(1/x_A)$ approximation that resums powers of $\alpha_S \ln(1/x_A)$. It is a priori not obvious that this description of the target, which requires small values of x_A , is valid for experiments at present energies. However, it has had success for many observables in the context of HERA [10] and RHIC [11].

The target is moving along the light-cone in the x^- direction, and the only component of its color current is J^- . With our choice of gauge $\mathcal{A}^+ = 0$, the current conservation law $[D_\mu, J^\mu] = \partial^+ J^- = 0$ implies that J^- does not depend on x^- . Therefore one writes

$$J^\mu(x^\nu) = \delta^{\mu-} J^-(x^+, \mathbf{x}) = \delta^{\mu-} T^c \rho_c(x^+, \mathbf{x}) \quad (11)$$

where we have introduced the color charge density of the target ρ_c . Solving the Yang-Mills equations $[D_\mu, F^{\mu\nu}] = J^\nu$ then leads to (see for instance [12])

$$A^\mu(x^\nu) = \delta^{\mu-} T^c \mathcal{A}_c^-(x^+, \mathbf{x}), \quad -\nabla^2 \mathcal{A}_c^-(x^+, \mathbf{x}) = \rho_c(x^+, \mathbf{x}). \quad (12)$$

The formal functional integration in (10) stands for the A^- integration.

In a scattering process, the outgoing state is obtained from the incoming state by action of the scattering matrix \mathcal{S} . When high-energy partons scatter off the CGC, the interaction is eikonal and the \mathcal{S} matrix acts on quarks and gluons as (see for example [13]):

$$\mathcal{S}|\mathbf{b}, i\rangle \otimes |\mathcal{A}\rangle = \sum_j W_F^{ij}[\mathcal{A}](\mathbf{b}) |\mathbf{b}, j\rangle \otimes |\mathcal{A}\rangle, \quad \mathcal{S}|\mathbf{x}, c\rangle \otimes |\mathcal{A}\rangle = \sum_d W_A^{cd}[\mathcal{A}](\mathbf{x}) |\mathbf{x}, d\rangle \otimes |\mathcal{A}\rangle, \quad (13)$$

where the phase shifts due to the interaction are described by W_F and W_A , the eikonal Wilson lines in the fundamental and adjoint representations respectively, corresponding to propagating quarks and gluons. They are given by

$$W_{F,A}[\mathcal{A}](\mathbf{x}) = \mathcal{P} \exp \left(ig_S \int dx^+ T_{F,A}^c \mathcal{A}_c^-(x^+, \mathbf{x}) \right) \quad (14)$$

with $T_{F,A}^a$ the generators of $SU(N_c)$ in the fundamental (F) or adjoint (A) representations and with \mathcal{P} denoting an ordering in x^+ . The Wilson lines resum powers of $g_S \mathcal{A}$ which is necessary as \mathcal{A} is a large classical field whose strength is of order $1/g_S$. It is manifest from (13) why the mixed representation introduced earlier is convenient: working with transverse space coordinates (instead of transverse momenta) provides eigenstates of the high-energy \mathcal{S} -matrix.

Coming back to our computation, the incoming and outgoing states are

$$|\Psi_{in}\rangle = |p, i, \alpha\rangle \otimes |\mathcal{T}\rangle, \quad |\Psi_{out}\rangle = \mathcal{S}|\Psi_{in}\rangle. \quad (15)$$

Using (7) and (13), it is straightforward to obtain (we now keep the \mathcal{A} dependence of the Wilson lines $W_{F,A}$ implicit)

$$|\Psi_{out}\rangle = \int D\mathcal{A} \Phi_{x_A}[\mathcal{A}] \int \frac{d^2b}{(2\pi)^2} e^{ip_\perp \cdot \mathbf{b}} \left(Z \sum_j [W_F(\mathbf{b})]_{ij} |p^+, \mathbf{b}, j, \alpha\rangle_0 \otimes |\mathcal{A}\rangle + \sum_{j\beta d\lambda} \int dk^+ \frac{d^2x}{(2\pi)^2} g_S \phi_{\alpha\beta}^\lambda(p, k^+, \mathbf{x} - \mathbf{b}) [T^c W_F(\mathbf{b})]_{ij} W_A^{cd}(\mathbf{x}) |(p^+ - k^+, \mathbf{b}, j, \beta); (k^+, \mathbf{x}, d, \lambda)\rangle_0 \otimes |\mathcal{A}\rangle \right). \quad (16)$$

In this formula, the quark-gluon contribution represents the first contribution pictured in Fig.1, for which the gluon is emitted before the interaction. The second contribution, for which the gluon is emitted after the interaction, is hidden in the quark contribution $Z|p^+, \mathbf{b}, i, \alpha\rangle_0$. To see that, let us write this in terms of $|p, i, \alpha\rangle$: from formula (7), and using the fact that the p_\perp dependence of $\phi_{\alpha\beta}^\lambda(p, k^+, \mathbf{x})$ is $\exp(ik^+ p_\perp \cdot \mathbf{x}/p^+)$, one obtains:

$$Z|p^+, \mathbf{b}, i, \alpha\rangle_0 = \int d^2p_\perp e^{-ip_\perp \cdot \mathbf{b}} |p, i, \alpha\rangle - \sum_{j\beta c\lambda} \int dk^+ \frac{d^2x}{(2\pi)^2} d^2b' \delta(\mathbf{b} - \mathbf{b}' - k^+(\mathbf{x} - \mathbf{b}')/p^+) g_S T_{ij}^c e^{ip_\perp \cdot (\mathbf{b}' - \mathbf{b})} \phi_{\alpha\beta}^\lambda(p, k^+, \mathbf{x} - \mathbf{b}') |(p^+ - k^+, \mathbf{b}', j, \beta); (k^+, \mathbf{x}, c, \lambda)\rangle_0. \quad (17)$$

One sees that the emission-after-interaction term arises with a minus sign. The dressed quark contribution $|p, i, \alpha\rangle$ does not contribute to gluon production, and can be removed from the final answer. Indeed, when computing gluon production, gluons which dress the final-state quark should not be included, as these are not actually produced.

Combining (16) and (17), the outgoing state can be simply rewritten as

$$|\Psi_{out}\rangle = \int D\mathcal{A} \Phi_{x_A}[\mathcal{A}] \sum_{j\beta c\lambda} \int dk^+ \frac{d^2x}{(2\pi)^2} \frac{d^2b}{(2\pi)^2} e^{ip_\perp \cdot \mathbf{b}} g_S \Phi_{\alpha\beta,ij}^{c\lambda}(p, k^+, \mathbf{x}, \mathbf{b}) |(p^+ - k^+, \mathbf{b}, j, \beta); (k^+, \mathbf{x}, c, \lambda)\rangle \otimes |\mathcal{A}\rangle \quad (18)$$

with

$$\Phi_{\alpha\beta,ij}^{c\lambda}(p, k^+, \mathbf{x}, \mathbf{b}) = \phi_{\alpha\beta}^\lambda(p, k^+, \mathbf{x} - \mathbf{b}) [T^d W_F(\mathbf{b}) W_A^{dc}(\mathbf{x}) - W_F(\mathbf{b} + k^+(\mathbf{x} - \mathbf{b})/p^+) T^c]_{ij} . \quad (19)$$

Once again, the different contributions contained in this wavefunction have a straightforward physical meaning: the term containing W_A corresponds to the interaction happening after the gluon emission while the contribution without W_A corresponds to the interaction taking place before.

C. The inclusive quark-gluon production cross-section $\sigma^{q\mathcal{T} \rightarrow qgX}$

From the outgoing state (18), one can now compute the production of a quark with momentum $q = (q^+, q_\perp)$ and a gluon with momentum $k = (k^+, k_\perp)$. The corresponding cross-section reads

$$\frac{d\sigma^{q\mathcal{T} \rightarrow qgX}}{d^3k d^3q} = \frac{1}{2N_c} \sum_{i\alpha} \langle \Psi_{out} | N_q(q) N_g(k) | \Psi_{out} \rangle \quad (20)$$

where we recall that i and α refer to the color and spin of the incoming quark of momentum $p = (p^+, p_\perp)$. In (20), the operators N_q and N_g are given by

$$N_q(q) = \sum_{j\beta} b_{j,\beta}^\dagger(q) b_{j,\beta}(q) , \quad N_g(k) = \sum_{a\lambda} a_{a,\lambda}^\dagger(k) a_{a,\lambda}(k) \quad (21)$$

in terms of the creation and annihilation operators introduced earlier in Section II-A. Let us rewrite the cross-section (20) using operators in the mixed representation (6):

$$\begin{aligned} \frac{d\sigma^{q\mathcal{T} \rightarrow qgX}}{d^3k d^3q} &= \frac{1}{2N_c} \int \frac{d^2x}{(2\pi)^2} \frac{d^2x'}{(2\pi)^2} \frac{d^2b}{(2\pi)^2} \frac{d^2b'}{(2\pi)^2} e^{ik_\perp \cdot (\mathbf{x}' - \mathbf{x})} e^{iq_\perp \cdot (\mathbf{b}' - \mathbf{b})} \\ &\sum_{a\lambda\alpha\beta ij} \langle \Psi_{out} | a_{a,\lambda}^\dagger(\mathbf{x}', k^+) b_{j,\beta}^\dagger(\mathbf{b}', q^+) a_{a,\lambda}(\mathbf{x}, k^+) b_{j,\beta}(\mathbf{b}, q^+) | \Psi_{out} \rangle , \end{aligned} \quad (22)$$

where \mathbf{x} and \mathbf{x}' (resp. \mathbf{b} and \mathbf{b}') represent now the transverse coordinates of the measured gluon (resp. quark) in the amplitude and the complex conjugate amplitude respectively. When computing the action of $a_{a,\lambda}$ and $b_{j,\beta}$ on $|\Psi_{out}\rangle$, one obtains

$$a_{a,\lambda}(\mathbf{x}, k^+) b_{j,\beta}(\mathbf{b}, q^+) |\Psi_{out}\rangle = g_S e^{ip_\perp \cdot \mathbf{b}} \delta(p^+ - k^+ - q^+) \int D\mathcal{A} \Phi_{x_A}[\mathcal{A}] \Phi_{\alpha\beta,ij}^{a\lambda}(p, k^+, \mathbf{x}, \mathbf{b}) |\mathcal{A}\rangle . \quad (23)$$

The function $\delta(p^+ - k^+ - q^+)$ in (23) shows that the longitudinal momenta are conserved during the high-energy eikonal scattering. However, this delta function at the level of the amplitude will lead to a factor $\delta(0)$ when computing the cross-section (22). This problem is related to the factor $\delta^{(3)}(0)$ present in the normalization of the state $|\Psi_{in}\rangle$, itself due to the fact that we are using plane waves. When computing a physical observable, this divergence usually goes away, as is the case for the two transverse dimensions. However, a $\delta(0)$ remains for the longitudinal direction precisely because longitudinal momenta are conserved by the interaction. Working with wave packets would solve the problem, and the appropriate prescription is to remove the factor $2\pi\delta(p^+ - k^+ - q^+)$ from the amplitude (23), and to put it back in the cross-section (22).

Denoting $z = k^+/p^+$ and using (23) in (22), one obtains the $q\mathcal{T} \rightarrow qgX$ cross-section ($\alpha_S = g_S^2/4\pi$):

$$\begin{aligned} \frac{d\sigma^{q\mathcal{T} \rightarrow qgX}}{d^3k d^3q} &= \alpha_S C_F \delta(p^+ - k^+ - q^+) \int \frac{d^2x}{(2\pi)^2} \frac{d^2x'}{(2\pi)^2} \frac{d^2b}{(2\pi)^2} \frac{d^2b'}{(2\pi)^2} e^{ik_\perp \cdot (\mathbf{x}' - \mathbf{x})} e^{i(q_\perp - p_\perp) \cdot (\mathbf{b}' - \mathbf{b})} \\ &\sum_{\lambda\alpha\beta} \phi_{\alpha\beta}^{\lambda*}(p, k^+, \mathbf{x}' - \mathbf{b}') \phi_{\alpha\beta}^\lambda(p, k^+, \mathbf{x} - \mathbf{b}) \left\{ S_{qg\bar{q}g}^{(4)}[\mathbf{b}, \mathbf{x}, \mathbf{b}', \mathbf{x}'; x_A] - S_{qg\bar{q}}^{(3)}[\mathbf{b}, \mathbf{x}, \mathbf{b}' + z(\mathbf{x}' - \mathbf{b}'); x_A] \right. \\ &\left. - S_{qg\bar{q}}^{(3)}[\mathbf{b} + z(\mathbf{x} - \mathbf{b}), \mathbf{x}', \mathbf{b}'; x_A] + S_{q\bar{q}}^{(2)}[\mathbf{b} + z(\mathbf{x} - \mathbf{b}), \mathbf{b}' + z(\mathbf{x}' - \mathbf{b}'); x_A] \right\} . \end{aligned} \quad (24)$$

In (24), we have introduced the following traces of products of Wilson lines:

$$S_{qg\bar{q}g}^{(4)}(\mathbf{b}, \mathbf{x}, \mathbf{b}', \mathbf{x}'; x_A) = \frac{1}{C_F N_c} \left\langle \text{Tr} \left(W_F(\mathbf{b}) W_F^\dagger(\mathbf{b}') T^d T^c \right) [W_A(\mathbf{x}) W_A^\dagger(\mathbf{x}')]^{cd} \right\rangle_{x_A}, \quad (25)$$

$$S_{qg\bar{q}}^{(3)}(\mathbf{b}, \mathbf{x}, \mathbf{b}'; x_A) = \frac{1}{C_F N_c} \left\langle \text{Tr} \left(W_F^\dagger(\mathbf{b}') T^c W_F(\mathbf{b}) T^d \right) W_A^{cd}(\mathbf{x}) \right\rangle_{x_A}, \quad (26)$$

$$S_{q\bar{q}}^{(2)}(\mathbf{b}, \mathbf{b}'; x_A) = \frac{1}{N_c} \left\langle \text{Tr} \left(W_F(\mathbf{b}) W_F^\dagger(\mathbf{b}') \right) \right\rangle_{x_A}, \quad (27)$$

and we have also denoted the average over the CGC wavefunction squared $|\Phi_{x_A}[\mathcal{A}]|^2$ using the following notation:

$$\int D\mathcal{A} |\Phi_{x_A}[\mathcal{A}]|^2 f[\mathcal{A}] = \langle f \rangle_{x_A}. \quad (28)$$

The quantities $S_{q\bar{q}}^{(2)}$, $S_{qg\bar{q}}^{(3)}$ and $S_{qg\bar{q}g}^{(4)}$ contain the QCD evolution toward small values of x_A . Some comments about formula (24) are in order.

- First one recovers the result of [6], except that in our case the interaction with the target is obtained by specific n -point functions, expressed in terms of Wilson lines that resum powers of $g_S \mathcal{A}$. These are to be averaged with the CGC wavefunction squared $|\Phi_{x_A}[\mathcal{A}]|^2$, whose x_A evolution resums powers of $\alpha_S \ln(1/x_A)$, in the leading- $\ln(1/x_A)$ approximation.
- Using the Fierz identities

$$[W_F(\mathbf{x})]_{ij} [W_F^\dagger(\mathbf{x})]_{kl} = \frac{1}{N_c} \delta_{il} \delta_{jk} + 2 W_A^{cd}(\mathbf{x}) T_{il}^c T_{kj}^d, \quad (29)$$

$$T_{ij}^c T_{kl}^c = \frac{1}{2} \delta_{il} \delta_{jk} - \frac{1}{2N_c} \delta_{ij} \delta_{kl}, \quad (30)$$

one obtains that $W_A^{cd}(\mathbf{x}) = 2 \text{Tr}(W_F^\dagger(\mathbf{x}) T^c W_F(\mathbf{x}) T^d)$ which shows that an adjoint Wilson line W_A is equivalent to two fundamental Wilson lines W_F . Therefore the quantities $S_{q\bar{q}}^{(2)}$, $S_{qg\bar{q}}^{(3)}$ and $S_{qg\bar{q}g}^{(4)}$ are 2-, 4- and 6-point functions with respect to the averaging (28). Using (29) and (30), one can also see that the singularities of $\phi_{\alpha\beta}^\lambda$ in (24) are cancelled when $\mathbf{x} = \mathbf{b}$ or $\mathbf{x}' = \mathbf{b}'$.

- Our result should be identical to that of [14], although this is not so straightforward to see, as their expression for the $q\mathcal{T} \rightarrow qgX$ cross-section is not as compact as our formula (24). This is probably because in [14], the Wilson lines are expressed in momentum space, where the interaction is not diagonal.

Let us finally consider the soft-gluon approximation $z \ll 1$. Not only does the wavefunction (9) simplify, but also many simplifications occur with the Wilson lines. Indeed using the Fierz identity to transform all the adjoint Wilson lines into fundamental ones, one obtains (if one also factorizes the remaining traces, meaning $\langle \text{Tr}(\cdot) \text{Tr}(\cdot) \rangle_{x_A} = \langle \text{Tr}(\cdot) \rangle_{x_A} \langle \text{Tr}(\cdot) \rangle_{x_A}$, we recover the expression of [5]):

$$\begin{aligned} S_{qg\bar{q}g}^{(4)}(\mathbf{b}, \mathbf{x}, \mathbf{b}', \mathbf{x}'; x_A) - S_{qg\bar{q}}^{(3)}(\mathbf{b}, \mathbf{x}, \mathbf{b}'; x_A) - S_{qg\bar{q}}^{(3)}(\mathbf{b}, \mathbf{x}', \mathbf{b}'; x_A) + S_{q\bar{q}}^{(2)}(\mathbf{b}, \mathbf{b}'; x_A) = & \frac{N_c}{2C_F} \left\langle \frac{1}{N_c} \text{Tr} \left(W_F(\mathbf{b}) W_F^\dagger(\mathbf{b}') \right) \right. \\ & - \frac{1}{N_c} \text{Tr} \left(W_F(\mathbf{b}) W_F^\dagger(\mathbf{x}) \right) \frac{1}{N_c} \text{Tr} \left(W_F(\mathbf{x}) W_F^\dagger(\mathbf{b}') \right) - \frac{1}{N_c} \text{Tr} \left(W_F(\mathbf{b}) W_F^\dagger(\mathbf{x}') \right) \frac{1}{N_c} \text{Tr} \left(W_F(\mathbf{x}') W_F^\dagger(\mathbf{b}') \right) \\ & \left. + \frac{1}{N_c} \text{Tr} \left(W_F(\mathbf{x}) W_F^\dagger(\mathbf{x}') \right) \frac{1}{N_c} \text{Tr} \left(W_F(\mathbf{b}) W_F^\dagger(\mathbf{b}') W_F(\mathbf{x}') W_F^\dagger(\mathbf{x}) \right) \right\rangle. \quad (31) \end{aligned}$$

The last term in this expression shows that even in the soft-gluon approximation, the dipole degrees of freedom (i.e. traces of two Wilson lines) are not sufficient to compute the dijet cross-section (24). This is an important difference with the case of single-particle production [15], for which using dipoles is enough, yielding the so-called k_T -factorization. For two-particle production, k_T -factorization cannot be used.

In the following we shall not consider the soft-gluon approximation, and work directly with the 2-, 4- and 6-point functions (27), (26) and (25). Indeed, we are interested in final-state configurations where the two particles are both detected in the forward hemisphere, with similar rapidities. By contrast, using a soft gluon would impose the constraint of a large rapidity between the two detected hadrons.

III. PERFORMING THE TARGET AVERAGES

In this section, we explain how to model the CGC wavefunction in order to perform the average (28) while taking into account the small- x QCD evolution. To compute the correlators $S_{q\bar{q}}^{(2)}$, $S_{qg\bar{q}}^{(3)}$ and $S_{gg\bar{q}g}^{(4)}$, we shall model the CGC wavefunction squared $|\Phi_{x_A}[\mathcal{A}]|^2$ using Gaussian-distributed sources. Then, following the approach of [16], we will work in the large- N_c limit which allows to easily implement the Balitsky-Kovchegov (BK) evolution, and also simplifies the analytic expression for the 6-point function.

A. A Gaussian distribution of sources

To compute the average (28), we use the following Gaussian distribution of sources

$$|\Phi_{x_A}[\mathcal{A}]|^2 = \exp\left(-\int d^2x d^2y dz^+ \frac{\rho_c(z^+, \mathbf{x})\rho_c(z^+, \mathbf{y})}{2\mu_{x_A}^2(z^+, \mathbf{x} - \mathbf{y})}\right) \quad (32)$$

where the color charge density ρ_c and the color field \mathcal{A} are simply related via formula (12). The variance $\mu_{x_A}^2$ is a function of x_A and characterizes the density of the color charges. With this Gaussian approximation, the 2-point and 4-point correlators (27) and (26) have been computed for arbitrary N_c (see for instance the Appendix A of [17]). They are given by

$$S_{q\bar{q}}^{(2)}(\mathbf{b}, \mathbf{b}'; x_A) = e^{-\frac{C_F}{2}\Gamma(\mathbf{b}-\mathbf{b}', x_A)}, \quad (33)$$

$$S_{qg\bar{q}}^{(3)}(\mathbf{b}, \mathbf{x}, \mathbf{b}'; x_A) = e^{-\frac{N_c}{4}[\Gamma(\mathbf{x}-\mathbf{b}, x_A) + \Gamma(\mathbf{x}-\mathbf{b}', x_A)] + \frac{1}{4N_c}\Gamma(\mathbf{b}-\mathbf{b}', x_A)}, \quad (34)$$

with the function $\Gamma(\mathbf{b}-\mathbf{b}', x_A)$ related to $\mu_{x_A}^2$ in the following way

$$\Gamma(\mathbf{b}-\mathbf{b}', x_A) = g_S^4 \int d^2x d^2y dz^+ \mu_{x_A}^2(z^+, \mathbf{x} - \mathbf{y}) [G_0(\mathbf{b} - \mathbf{x}) - G_0(\mathbf{b}' - \mathbf{x})][G_0(\mathbf{y} - \mathbf{b}) - G_0(\mathbf{y} - \mathbf{b}')], \quad (35)$$

where G_0 is the two-dimensional massless propagator

$$G_0(\mathbf{x}) = \int_{|\mathbf{k}| > \Lambda_{QCD}} \frac{d^2k}{(2\pi)^2} \frac{e^{i\mathbf{k}\cdot\mathbf{x}}}{\mathbf{k}^2}. \quad (36)$$

The last correlator needed for our study has a more complicated structure. Following the derivation of the 4-point function in [17], it is easy to see that the problem of computing the six point function (25) can be reduced to the diagonalisation of a 6×6 matrix. Note that in the recent publication [18], a method to compute any n -point function is presented. As already mentioned, only the large- N_c limit is used in the implementation of the small- x QCD evolution. Therefore, computing the exact structure of the 6-point function $S_{qg\bar{q}g}^{(4)}$ is of no interest for the present study. We only give the large- N_c result

$$S_{qg\bar{q}g}^{(4)}(\mathbf{b}, \mathbf{x}, \mathbf{b}', \mathbf{x}'; x_A) = e^{-\frac{N_c}{4}[\Gamma(\mathbf{x}-\mathbf{b}, x_A) + \Gamma(\mathbf{x}'-\mathbf{b}', x_A) + \Gamma(\mathbf{x}-\mathbf{x}', x_A)]}. \quad (37)$$

This will be used along with formula (33) and the large- N_c limit of formula (34). Note that these expression should be understood for scattering at fixed impact parameter, which is why they feature one less independent variable than expected. We will assume in the following that the impact-parameter dependence of the correlators factorizes.

B. Evolving the MV model with the BK equation

Let us now explain the strategy to evaluate the function $\Gamma(\mathbf{r}, x_A)$, in terms of which all the correlators (33), (34) and (37) could be written. We will use the fact that, under the assumption (32) that the CGC wavefunction is Gaussian, the large- N_c limit implies the following result

$$\left\langle \text{Tr}\left(W_F(\mathbf{b})W_F^\dagger(\mathbf{b}')\right)\text{Tr}\left(W_F(\mathbf{x})W_F^\dagger(\mathbf{x}')\right) \right\rangle_{x_A} = \left\langle \text{Tr}\left(W_F(\mathbf{b})W_F^\dagger(\mathbf{b}')\right) \right\rangle_{x_A} \left\langle \text{Tr}\left(W_F(\mathbf{x})W_F^\dagger(\mathbf{x}')\right) \right\rangle_{x_A}. \quad (38)$$

This significantly simplifies the high-energy QCD evolution equations. Indeed, when considering the Balitsky hierarchy of equations for the n -point correlators, (which is a rewriting the JIMWLK functional equation for the evolution of $|\Phi_{x_A}[\mathcal{A}]|^2$ with x_A), the factorization (38) reduces the QCD evolution to a single closed non-linear equation for $S_{q\bar{q}}^{(2)}(\mathbf{b}, \mathbf{b}'; x_A)$, known as the BK equation [7]. In this work, we consider the impact-parameter independent version

$$\frac{dS_{q\bar{q}}^{(2)}(\mathbf{b} - \mathbf{b}'; x)}{d \ln(1/x)} = \bar{\alpha} \int \frac{d^2 z}{2\pi} \frac{(\mathbf{b} - \mathbf{b}')^2}{(\mathbf{b} - \mathbf{z})^2 (\mathbf{z} - \mathbf{b}')^2} \left(S_{q\bar{q}}^{(2)}(\mathbf{b} - \mathbf{z}; x) S_{q\bar{q}}^{(2)}(\mathbf{z} - \mathbf{b}'; x) - S_{q\bar{q}}^{(2)}(\mathbf{b} - \mathbf{b}'; x) \right) \quad (39)$$

with $\bar{\alpha} = \alpha_S N_c / \pi$. From formula (35), the solution of the BK equation (39) gives $\Gamma(\mathbf{b} - \mathbf{b}', x_A)$, which allows to compute all the n -point functions needed for the calculation of the $q\mathcal{T} \rightarrow qgX$ cross-section.

As the initial condition, we shall use the McLerran-Venugopalan (MV) model [8] for $\Gamma(\mathbf{r}, x_0)$. It is obtained from a Gaussian average of the type (32), with $\mu_{x_0}^2(z^+, \mathbf{x}) = \delta(\mathbf{x}) \mu_{x_0}^2(z^+)$:

$$\Gamma(\mathbf{r}, x_0) = g_S^4 \mathbf{r}^2 \left(\int dz^+ \mu_{x_0}^2(z^+) \right) \int_{|\mathbf{r}| \Lambda_{QCD}}^{\infty} dk \frac{1 - J_0(k)}{\pi k^3} . \quad (40)$$

For $|\mathbf{r}| \Lambda_{QCD} \ll 1$, the remaining integral behaves as $-\ln(\mathbf{r}^2 \Lambda_{QCD}^2) / (8\pi)$. This leads to the MV model:

$$\Gamma(\mathbf{r}, x_0) = \frac{1}{2C_F} \mathbf{r}^2 Q_{s_0}^2 \ln \left(e + \frac{1}{\mathbf{r}^2 \Lambda_{QCD}^2} \right), \quad Q_{s_0}^2 = \frac{g_S^4 C_F}{4\pi} \left(\int dz^+ \mu_{x_0}^2(z^+) \right) \quad (41)$$

where Q_{s_0} is the initial saturation scale, at $x = x_0$. In practice, we choose to start the BK evolution at $x_0 = 0.01$, which is small enough to justify using the MV model. For a target Gold or Lead nucleus, $2\pi Q_{s_0}^2 = 2 \text{ GeV}^2$ is appropriate at $x_0 = 0.01$ (we use the same value as in [16], our saturation scales differ by a factor $\sqrt{2\pi}$). For that moderately small value of x , the MV model gives reasonable results in heavy ion collisions at RHIC [11]. For $x < x_0$, the quantum evolution effects are then implemented by the BK evolution.

It is known that the BK equation (39), equipped with the leading-logarithmic [19] Balitsky-Fadin-Kuraev-Lipatov (BFKL) kernel $\chi(\gamma) = 2\psi(1) - \psi(\gamma) - \psi(1 - \gamma)$ (in Mellin space), leads to an increase of the saturation scale that goes as

$$Q_s^2(x) = Q_{s_0}^2 \left(\frac{x_0}{x} \right)^{v\bar{\alpha}} \quad \text{with } v = \chi'(\gamma_c) = \frac{\chi(\gamma_c)}{\gamma_c} = 4.88 \quad (\gamma_c = 0.6275) . \quad (42)$$

In practice however, the appropriate saturation exponent is $Q_s^2 \sim x^{-\lambda}$ with $\lambda \simeq 0.25$, and this discrepancy is understood in terms of subleading logarithms [20]. In this work, in order to mimic to correct evolution of the saturation scale with x , we impose the unphysical value $\bar{\alpha} = 0.05$ when solving the BK equation (39). This is a simple way to account for the unknown next-leading effects, while staying compatible with experimental observations.

C. Expression for the cross-section

We now come back to the expression (24) for the $q\mathcal{T} \rightarrow qgX$ cross-section, which can be simplified using the results (33), (34) and (37) for the 2-, 4- and 6-point functions (27), (26) and (25) in the large- N_c limit. Let us first factor out some prefactors:

$$\frac{d\sigma^{q\mathcal{T} \rightarrow qgX}}{d^3 k d^3 q} = \alpha_S C_F \delta(p^+ - k^+ - q^+) M(p, k, q) . \quad (43)$$

Changing the integration variables to $\mathbf{u} = \mathbf{x} - \mathbf{b}$, $\mathbf{v} = z\mathbf{x} + (1-z)\mathbf{b}$, $\mathbf{u}' = \mathbf{x}' - \mathbf{b}'$, and $\mathbf{v}' = z\mathbf{x}' + (1-z)\mathbf{b}'$, one writes

$$\begin{aligned} M(p, k, q) = & \int \frac{d^2 u}{(2\pi)^2} \frac{d^2 u'}{(2\pi)^2} e^{i\kappa \cdot (\mathbf{u}' - \mathbf{u})} \sum_{\lambda\alpha\beta} \phi_{\alpha\beta}^{\lambda*}(p, k^+, \mathbf{u}') \phi_{\alpha\beta}^{\lambda}(p, k^+, \mathbf{u}) \int \frac{d^2 v}{(2\pi)^2} \frac{d^2 v'}{(2\pi)^2} e^{i\Delta \cdot (\mathbf{v}' - \mathbf{v})} \\ & \left(e^{-\frac{N_c}{4} [\Gamma(\mathbf{u}, x_A) + \Gamma(\mathbf{u}', x_A) + \Gamma(\mathbf{v} - \mathbf{v}' + (1-z)(\mathbf{u} - \mathbf{u}'), x_A)]} - e^{-\frac{N_c}{4} [\Gamma(\mathbf{u}, x_A) + \Gamma(\mathbf{v} - \mathbf{v}' + (1-z)\mathbf{u}, x_A)]} \right. \\ & \left. - e^{-\frac{N_c}{4} [\Gamma(\mathbf{u}', x_A) + \Gamma(\mathbf{v}' - \mathbf{v} + (1-z)\mathbf{u}', x_A)]} + e^{-\frac{N_c}{4} \Gamma(\mathbf{v} - \mathbf{v}', x_A)} \right) \end{aligned} \quad (44)$$

where we have introduced the following transverse momenta

$$\kappa = (1-z)k_{\perp} + z(p_{\perp} - q_{\perp}), \quad \Delta = k_{\perp} + q_{\perp} - p_{\perp} . \quad (45)$$

In (44), the transverse momentum transferred during the collision Δ is Fourier conjugate to $\mathbf{v} - \mathbf{v}'$, while κ , which characterizes the invariant mass of the final-state qg system, is Fourier conjugate to $\mathbf{u} - \mathbf{u}'$.

We now change the integration variables \mathbf{v} and \mathbf{v}' to $\mathbf{r} = \mathbf{v} - \mathbf{v}'$, and $\mathbf{B} = (\mathbf{v} + \mathbf{v}')/2$. The integration over \mathbf{B} represents the impact parameter integration. Following our approximation that in the correlators the \mathbf{B} dependence factorizes (and is not explicitly indicated), one has $\int d^2B(1 - S) = S_T(1 - S)$ and the \mathbf{B} integration simply yields the normalization factor S_T , which characterizes the transverse area of the target. One obtains

$$M(p, k, q) = \frac{S_T}{4\pi^2} \int \frac{d^2u}{(2\pi)^2} \frac{d^2u'}{(2\pi)^2} \sum_{\lambda\alpha\beta} \phi_{\alpha\beta}^{\lambda*}(p, k^+, \mathbf{u}') \phi_{\alpha\beta}^\lambda(p, k^+, \mathbf{u}) \int \frac{d^2r}{(2\pi)^2} e^{-i\Delta \cdot \mathbf{r}} e^{-\frac{N_c}{4}\Gamma(\mathbf{r}, x_A)} \\ \left(e^{i(p_\perp - q_\perp) \cdot (\mathbf{u}' - \mathbf{u})} e^{-\frac{N_c}{4}[\Gamma(\mathbf{u}, x_A) + \Gamma(\mathbf{u}', x_A)]} - e^{i\kappa \cdot \mathbf{u}' - i(p_\perp - q_\perp) \cdot \mathbf{u}} e^{-\frac{N_c}{4}[\Gamma(\mathbf{u}, x_A)]} \right. \\ \left. - e^{-i\kappa \cdot \mathbf{u} + i(p_\perp - q_\perp) \cdot \mathbf{u}'} e^{-\frac{N_c}{4}[\Gamma(\mathbf{u}', x_A)]} + e^{i\kappa \cdot (\mathbf{u}' - \mathbf{u})} \right). \quad (46)$$

Finally, performing the Fourier transforms back to momentum space, the cross-section can be written in the following compact form:

$$\frac{d\sigma^{qT \rightarrow qgX}}{d^3k d^3q} = S_T \frac{\alpha_S C_F}{4\pi^2} \delta(p^+ - k^+ - q^+) \sum_{\lambda\alpha\beta} \left| I_{\alpha\beta}^\lambda(p, k^+, p_\perp - q_\perp; x_A) - \psi_{\alpha\beta}^\lambda(p, k^+, \kappa) \right|^2 F_{x_A}(\Delta) \quad (47)$$

where we recall that $\psi_{\alpha\beta}^\lambda$ is the $q \rightarrow qg$ wavefunction (5) in momentum space, and with

$$I_{\alpha\beta}^\lambda(p, k^+, \kappa; x_A) = \int \frac{d^2u}{(2\pi)^2} e^{-i\kappa \cdot \mathbf{u}} e^{-\frac{N_c}{4}\Gamma(\mathbf{u}, x_A)} \phi_{\alpha\beta}^\lambda(p, k^+, \mathbf{u}). \quad (48)$$

We have also introduced the so-called unintegrated gluon distribution $F_{x_A}(\Delta)$, which is simply the Fourier transform of the 2-point function $S_{q\bar{q}}^{(2)}$:

$$F_{x_A}(\Delta) = \int \frac{d^2r}{(2\pi)^2} e^{-i\Delta \cdot \mathbf{r}} e^{-\frac{N_c}{4}\Gamma(\mathbf{r}, x_A)}. \quad (49)$$

It is important to stress that $F_{x_A}(\Delta)$ is not the usual unintegrated distribution defined in the leading-twist approximation of perturbative QCD, but it is rather an all-twist gluon distribution, as multiple scattering are taken into account. Although they coincide for large momentum, $F_{x_A}(\Delta)$ contains more information, as it is also properly defined in the infrared (meaning for $\Delta^2 < Q_s^2$). Note that the numerical Fourier transformation in (49) suffers from a positivity problem and features oscillations for large momenta [21]. This is due to the infrared behavior of the initial condition $\Gamma(\mathbf{r}, x_0)$, and the problem is carried to lower values of x_A by the BK evolution. To cure this, we substituted the $\Theta(k - |\mathbf{r}|\Lambda_{QCD})$ function in (40) by the smooth cutoff function $2 \arctan[(k/|\mathbf{r}|\Lambda_{QCD})^2]/\pi$. This modification of the infrared regularisation does not influence the results provided F_{x_A} is evaluated for values of $|\Delta|$ much bigger than Λ_{QCD} , and this will be the case

Finally let us insist that, as already mentioned, the unintegrated gluon distribution F_{x_A} is not enough to characterize the CGC, and for the process considered here, more information is needed to compute the cross-section. It is contained in the modified wavefunction $I_{\alpha\beta}^\lambda$:

$$I_{\alpha\beta}^\lambda(p, k^+, \kappa; x_A) = \frac{1}{\sqrt{k^+}} \begin{cases} \sqrt{2}\varepsilon_\perp^1 \cdot G_{x_A}(\kappa - zp_\perp) [\delta_{\alpha-}\delta_{\beta-} + (1-z)\delta_{\alpha+}\delta_{\beta+}] + H_{x_A}(\kappa - zp_\perp) \delta_{\alpha+}\delta_{\beta-} & \lambda = 1 \\ \sqrt{2}\varepsilon_\perp^2 \cdot G_{x_A}(\kappa - zp_\perp) [\delta_{\alpha+}\delta_{\beta+} + (1-z)\delta_{\alpha-}\delta_{\beta-}] - H_{x_A}(\kappa - zp_\perp) \delta_{\alpha-}\delta_{\beta+} & \lambda = 2 \end{cases} \quad (50)$$

given in terms of the functions

$$G_{x_A}(\kappa) = mz \frac{\kappa}{|\kappa|} \int du e^{-\frac{N_c}{4}\Gamma(u, x_A)} u K_1(mzu) J_1(|\kappa|u), \quad (51)$$

$$H_{x_A}(\kappa) = mz^2 \int du e^{-\frac{N_c}{4}\Gamma(u, x_A)} u K_0(mzu) J_0(|\kappa|u), \quad (52)$$

that contain the rest of the x_A dependence. The functions F_{x_A} , G_{x_A} (which is a two-dimensional vector) and H_{x_A} are all obtained from the function $\Gamma(u = |\mathbf{u}|, x_A)$, itself obtained by solving the BK equation.

IV. AZIMUTHAL ANGLE CORRELATIONS IN d - Au COLLISIONS

In this final section we consider the inclusive two-particle spectrum for the process $h\mathcal{T} \rightarrow h_1 h_2 X$ and, as an application, we study the correlations in azimuthal angle between the measured particles h_1 and h_2 , which are both detected at forward rapidities. We consider deuteron-gold collisions at RHIC center-of-mass energies ($\sqrt{s} = 200$ GeV/nucleon) and investigate the suppression of the back-to-back peak as a function of the transverse momenta and rapidities of the two particles.

A. The inclusive quark-gluon production cross-section $\sigma^{h\mathcal{T} \rightarrow qgX}$

Let us denote P^+ the momentum of the hadron h . To obtain the cross-section $\sigma^{h\mathcal{T} \rightarrow qgX}$ from the partonic cross-section $\sigma^{q\mathcal{T} \rightarrow qgX}$, one can use the collinear factorization of the quark density inside the hadron $q(p^+/P^+, \mu^2)$ where μ^2 is the factorization scale:

$$\frac{d\sigma^{h\mathcal{T} \rightarrow qgX}}{d^3k d^3q} = \int dx q(x, \mu^2) \frac{d\sigma^{q\mathcal{T} \rightarrow qgX}}{d^3k d^3q}(p^+ = xP^+, p_\perp = 0). \quad (53)$$

Indeed, we are interested in measurements that probe only large values of p^+/P^+ . By contrast, partons with small fraction of momentum are probed inside the target, and it cannot be described by a single gluon distribution (as obvious from formula (24) for instance). We shall later use the factorization scale $\mu^2 = \Delta^2$ which is the transverse momentum transferred during the collision, and it is supposed to be large to justify our perturbative calculations.

As a function of k_\perp and Δ , the $\sigma^{h\mathcal{T} \rightarrow qgX}$ cross-section reads

$$\frac{d\sigma^{h\mathcal{T} \rightarrow qgX}}{d^2k_\perp d^2q_\perp dy_k dy_q} = S_T \frac{\alpha_S C_F}{4\pi^2} (1-z) x_h q(x_h, \Delta^2) k^+ \sum_{\lambda\alpha\beta} |I_{\alpha\beta}^\lambda(p, k^+, k_\perp - \Delta; x_A) - \psi_{\alpha\beta}^\lambda(p, k^+, k_\perp - z\Delta)|^2 F_{x_A}(\Delta) \quad (54)$$

where in $I_{\alpha\beta}^\lambda$ and $\psi_{\alpha\beta}^\lambda$, p should be understood as ($p^+ = q^+ + k^+$, $p_\perp = 0$). Also, z now stands for $z = k^+ / (k^+ + q^+)$ and we have denoted $x_h = (k^+ + q^+) / P^+$, the fraction of momentum of the probed quark inside the incoming hadron. Note that similarly, there is conservation of momentum along the x^- direction and one has $x_A = (k^- + q^-) / P^-$ where P^- is the momentum of the incoming target. In terms of the rapidity of the quark y_q , the rapidity of the gluon y_k and the center of mass energy \sqrt{s} , one has:

$$z = \frac{|k_\perp| e^{y_k}}{|k_\perp| e^{y_k} + |q_\perp| e^{y_q}}, \quad x_h = \frac{|k_\perp| e^{y_k} + |q_\perp| e^{y_q}}{\sqrt{s}}, \quad x_A = \frac{|k_\perp| e^{-y_k} + |q_\perp| e^{-y_q}}{\sqrt{s}}. \quad (55)$$

It is clear that in order to have $x_h \lesssim 1$ and $x_A \ll 1$, one needs forward rapidities, in the hemisphere in which the hadron h fragments, where y_q and y_k are positive.

In this work, we do not take into account the fragmentation of the final-state quark and gluon into hadrons. Since we are interested in azimuthal angle correlations, fragmentation does not play an important role. Also, we do not include in the process $h\mathcal{T} \rightarrow h_1 h_2 X$, the contributions of the gluon-initiated subprocesses $g\mathcal{T} \rightarrow q\bar{q}X$ and $g\mathcal{T} \rightarrow ggX$. Measurements at forward rapidities at RHIC energies involve values of x_h so high that they are only sensitive to the valence quarks. In the case of the LHC, it is likely that one also needs to account for the gluon-initiated subprocesses.

In order to simplify the numerical computations, we shall work with massless quarks. Using $m = 0$ yields

$$G_{x_A}(k_\perp) = \frac{k_\perp}{|k_\perp|} \int du e^{-\frac{N_c}{4}\Gamma(u, x_A)} J_1(|k_\perp|u), \quad H_{x_A}(k_\perp) = 0 \quad (56)$$

and in (54), the summation over the quark and gluon spins and polarizations becomes

$$k^+ \sum_{\lambda\alpha\beta} |I_{\alpha\beta}^\lambda(p, k^+, k_\perp - \Delta; x_A) - \psi_{\alpha\beta}^\lambda(p, k^+, k_\perp - z\Delta)|^2 = 2 [1 + (1-z)^2] \left| G_{x_A}(k_\perp - \Delta) - \frac{k_\perp - z\Delta}{|k_\perp - z\Delta|^2} \right|^2. \quad (57)$$

In Fig.2, we display the functions F_{x_A} and G_{x_A} (in the massless case) obtained from the BK evolution. More precisely, the function $\Delta^2 F_{x_A}(\Delta)$ is displayed in Fig.2a and as is well-known, it is peaked for $\Delta^2 \simeq Q_s^2$, and therefore as x_A decreases the peak travels towards higher momenta. The evolution is however quite slow, considering the small value of the saturation exponent λ . The function $1 - k_\perp \cdot G_{x_A}(k_\perp)$ is represented in Fig.2b, it decreases from 1 to 0 as k_\perp^2 increases, and the front travels to higher momenta as x_A decreases.

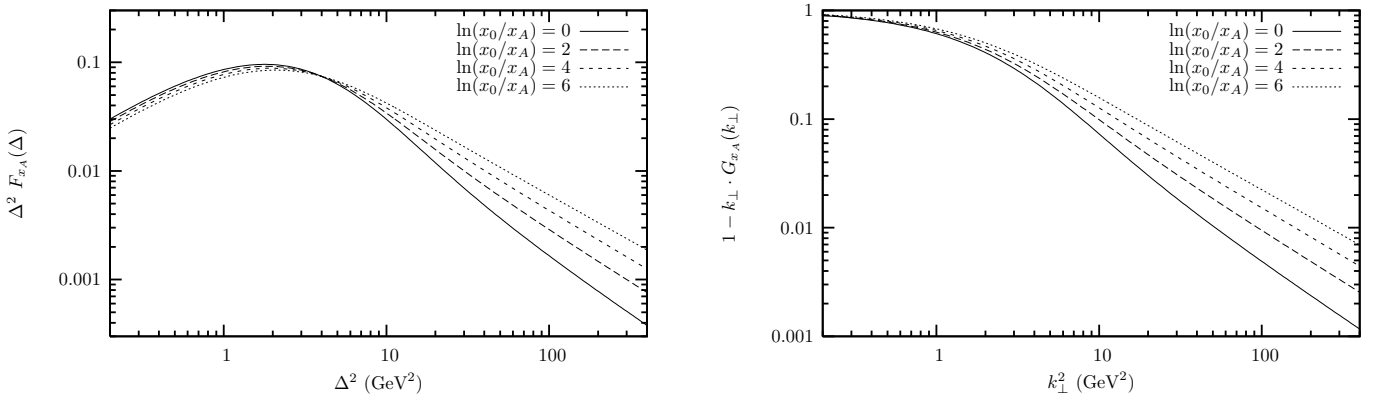


FIG. 2: Left plot: the dimensionless unintegrated gluon distribution $\Delta^2 F_{x_A}(\Delta)$ as a function of Δ^2 (see formula (49)). Right plot: the dimensionless quantity $1 - k_\perp \cdot G_{x_A}(k_\perp)$ as a function of k_\perp^2 (see formula (56), in the massless case). The curve for $x_A = x_0 = 0.01$ is obtained from the MV initial condition (40). The evolution towards smaller values of x_A is obtained with the BK equation (39), and is shown over 6 units of $\ln(x_0/x_A)$.

At this point, it is easy to recover the perturbative limit of the inclusive two-particle spectrum (54): for $|k_\perp| \gg Q_s$, $G_{x_A}(k_\perp) = k_\perp/|k_\perp|^2$ leads to k_T -factorization. For $|\Delta| \gg Q_s$ one has $F_{x_A}(\Delta) = Q_s^2(x_A)/(\pi\Delta^4)$ [22] which yields

$$\frac{d\sigma_{pQCD}^{hT \rightarrow qqX}}{d^2k_\perp d^2q_\perp dy_k dy_q} = S_T \frac{\alpha_S C_F}{2\pi^3} \frac{(1-z)^3 [1 + (1-z)^2] Q_s^2(x_A)}{(k_\perp - \Delta)^2 \Delta^2 (k_\perp - z\Delta)^2} x_h q(x_h, \Delta^2). \quad (58)$$

B. An application: azimuthal angle decorrelations

We will now use the inclusive two-particle spectrum (54) to investigate the process $hT \rightarrow h_1 h_2 X$, and in particular the cross-section as a function of $\Delta\phi = \phi_1 - \phi_2$, the difference in azimuthal angles of the two measured particles h_1 and h_2 . We will study the normalized $\Delta\phi$ distribution

$$\frac{1}{\sigma} \frac{d\sigma}{d\Delta\phi} \equiv \left(\frac{d\sigma^{hT \rightarrow h_1 h_2 X}}{dp_{T_1} dp_{T_2} dy_1 dy_2} \right)^{-1} \frac{d\sigma^{hT \rightarrow h_1 h_2 X}}{dp_{T_1} dp_{T_2} dy_1 dy_2 d\Delta\phi} \quad (59)$$

where (p_{T_1}, ϕ_1) and (p_{T_2}, ϕ_2) are the transverse momenta of the measured hadrons and y_1 and y_2 are their rapidities. Our results can be applied to d - Au collisions at RHIC, and to compute x_h and x_A we will use $\sqrt{s} = 200$ GeV.

A given final-state configuration can be obtained in two possible ways from the $hT \rightarrow qqX$ process, depending on which particle (1 or 2) comes from the quark and which comes from the gluon. While x_h and x_A are the same in both situations, it is not the case of z (which is changed into $1-z$), and therefore the cross-section (54) is not symmetric with respect to the two situations, as it is a decreasing function of z . Let us choose to label the particles such that $p_{T_1} e^{y_1} > p_{T_2} e^{y_2}$. If the quark (resp. gluon) is the particle 1, then $z < 1/2$ (resp. $z > 1/2$). This shows that, for similar transverse momenta $p_{T_1} \sim p_{T_2}$, the favored configuration is the one where the quark is the most forward particle; this is especially true when $y_1 - y_2$ is large. In any case, we take into account both situations.

The massless quark approximation is valid when $(k_\perp - z\Delta)^2 \gg m^2$, therefore we will stay away from the situation $y_1 = y_2$, because when $\Delta\phi = 0$ it leads $(k_\perp - z\Delta)^2 = 0$. In this situation the factor $(k_\perp - z\Delta)^{-2}$ in (57) should actually be replaced by $1/m^2$; there is an increase of the cross-section when $\Delta\phi \simeq 0$ and $y_1 \simeq y_2$, which corresponds to the quark and the gluon being collinear. Also we shall not consider the situation $p_{T_1} = p_{T_2}$ which implies that $\Delta^2 = 0$ for $\Delta\phi = \pi$. Indeed, we would like to work with $|\Delta| \gg \Lambda_{QCD}$.

As can be seen from the kinematics (55), the most forward of the two particles essentially determines the value of x_h while the most central one determines the value of x_A . In order to study the effect of the CGC evolution, the ideal situation would be to keep x_h fixed and to vary x_A . In practice, this is better realized by fixing the rapidity and momentum of the most forward particle and by varying the kinematics of the other. Note that doing the opposite would emphasize the x_h evolution of $q(x_h, \Delta^2)$, rather than focus on the x_A evolution of F_{x_A} and G_{x_A} . Moreover, the cross-section (54) is quite sensitive to choice of factorization scale in the quark density, so it is better to keep x_h constant. Note that varying the rapidities at fixed $y_1 - y_2$ would keep the product $x_h x_A$ constant, and would force a competition between the evolution of $q(x_h, \Delta^2)$ with increasing x_h and the CGC evolution with decreasing x_A .

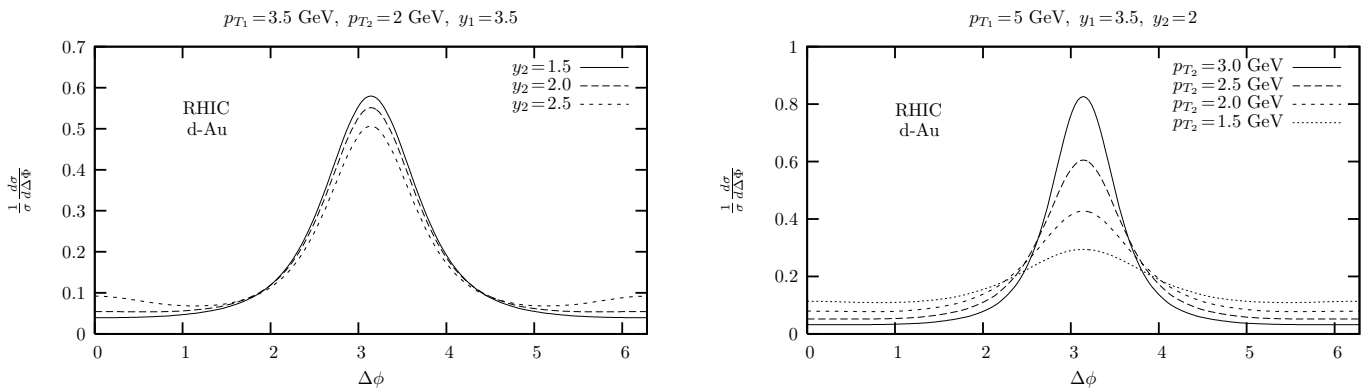


FIG. 3: The $\Delta\phi$ spectrum (59) in two situations for the RHIC energy $\sqrt{s} = 200$ GeV/nucleon. Fig.3a: $p_{T1} = 3.5$ GeV, $p_{T2} = 2$ GeV, $y_1 = 3.5$ and y_2 is varied from 1.5 to 2.5. Fig.3b: $p_{T1} = 5$ GeV, $y_1 = 3.5$, $y_2 = 2$ and p_{T2} is varied 1.5 GeV to 3 GeV. In both cases, the correlation in azimuthal angle is suppressed as the value of x_A probed in the process decreases. Varying p_{T2} at fixed y_2 is much more efficient as the ratio p_{T2}/Q_s varies over a larger range.

In Fig.3a, we have studied the $\Delta\phi$ spectrum (59) in the situation in which $p_{T1} = 3.5$ GeV, $p_{T2} = 2$ GeV, $y_1 = 3.5$ and y_2 is varied from 1.5 to 2.5. As y_2 increases, the value of x_A decreases and the suppression of the azimuthal correlation is more important. However the effect is quite small, because the increase of the saturation scale with decreasing x_A is rather slow. In Fig.3b, we investigate the situation for which $p_{T1} = 5$ GeV, $y_1 = 3.5$, $y_2 = 2$ and p_{T2} is varied 1.5 GeV to 3 GeV. As p_{T2} decreases, it gets closer to the saturation scale Q_s (which also slightly increases as x_A decreases), and the suppression of the azimuthal correlation increases. Varying p_{T2} at fixed y_2 allows to probe the ratio p_{T2}/Q_s over a larger range, so the effect is much bigger than when varying y_2 at fixed p_{T2} .

Experimental measurements of two-particle correlations in azimuthal angle have been performed at RHIC in d -Au collisions [23] by the PHENIX and STAR collaborations. Our predictions for the fully differential cross section are not directly comparable with the data. One would have to carry out a number of integrations over the kinematic variables, while properly taking into account the kinematic cuts applied by the experiments for the different measurements, but this goes beyond the scope of this work. Nevertheless the exploratory measurements of STAR with π^0 at forward rapidity and charged hadrons at mid rapidity are qualitatively consistent with a suppression of the back-to-back peak with respect to p - p collisions. By contrast, the measurements of PHENIX do not show any evidence of a suppression of the back-to-back peak, but they probe values of x_A which are bigger than 0.01. It may very well be that the CGC picture breaks down for values of x_A bigger than 0.01, and it justifies our choice not to start the small- x_A evolution at a higher value.

In Fig.4, the $\Delta\Phi$ spectrum (59) is plotted for the same situations as in Fig.3, but with the LHC heavy-ion energy $\sqrt{s} = 5.5$ TeV/nucleon. Assuming similar possibilities for the ALICE detector, compared to RHIC detectors, the final-state kinematics are unchanged, and as a result the values of x_A probed in the process are much smaller at the LHC (typically $x_A \sim 5 \cdot 10^{-5}$), compared to RHIC (typically $x_A \sim 10^{-3}$). One sees that in both cases, the azimuthal angle decorrelation behaves as a function of y_2 and p_{T2} as in Fig.3, but as indicated by the vertical scale, the spectrum is globally more suppressed and the peak is also slightly broader. Let us warn that those conclusions are only qualitative, as our calculation is really only suited for RHIC where the $q \rightarrow qg$ process is predominant. The values of x_h probed at the LHC (typically $x_h \sim 0.02$ compared to $x_h \sim 0.5$ at RHIC) are such that the gluon-initiated processes $g \rightarrow q\bar{q}$ and $g \rightarrow gg$ (not included in our calculation) will dominate the cross-section.

V. CONCLUSIONS

Let us summarize our main results. We computed forward inclusive dijet production $q\mathcal{T} \rightarrow qgX$ in the scattering of a quark off a Color Glass Condensate. The two-particle spectrum (24) was expressed in terms of correlators of Wilson lines. With the Gaussian CGC wavefunction (32), we could compute the correlators in terms of a single function, which in practice is obtained (in the large- N_c limit) by solving the BK equation (39) with the MV initial condition (40). We applied our expression (47) to the process $h\mathcal{T} \rightarrow h_1 h_2 X$, the inclusive production of two particles h_1 and h_2 at forward rapidities, in the direction of the dilute hadron h . As an application of formula (54), we studied the azimuthal angle correlation in d -Au collisions. While our results for the fully differential spectrum (59) are not yet comparable with the data, we obtain a qualitative agreement.

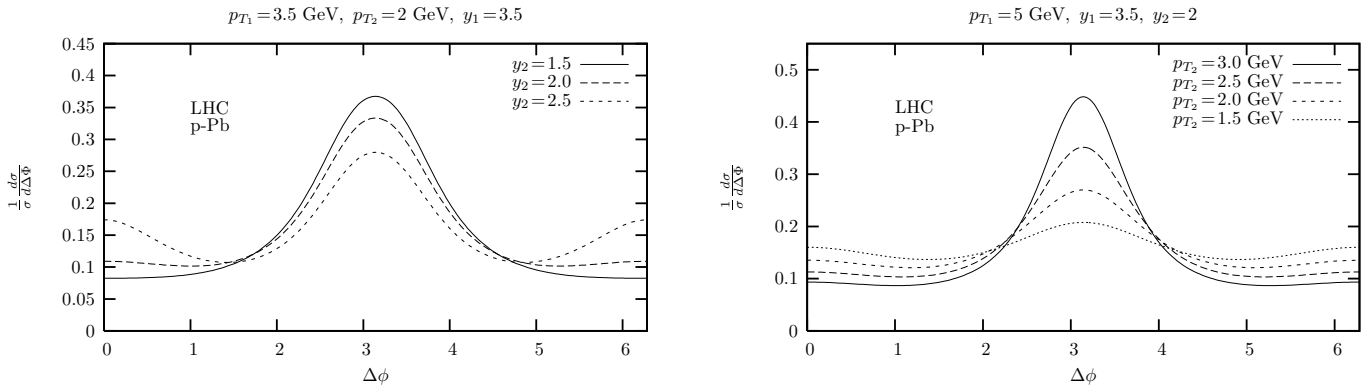


FIG. 4: The $\Delta\phi$ spectrum (59) in the two situations studied in Fig.3, but for the LHC energy $\sqrt{s}=5.5$ TeV/nucleon, resulting in probing much smaller values of x_A . In both cases, the correlation in azimuthal angle varies as a function of y_2 and p_{T_2} as in Fig.3, but globally the azimuthal correlation is more suppressed (see the vertical axis) and the peak is less pronounced.

However, if the CGC discovery at RHIC is to be promoted to the same level than that of the quark-gluon plasma [24], then the qualitative agreements should be made quantitative. This has been done in the case of single particle production at forward rapidities in d - Au collisions [25]. For azimuthal correlations, this paper represents a first step, but more efforts are required, on both the experimental and theoretical sides. Other d - Au runs at RHIC in the future would certainly be of interest, for instance the accessible range in rapidity could be improved.

The present calculation takes into account the effects of the non-linear QCD evolution at small- x . However, since the validity of the CGC picture requires $x < 0.01$, with the RHIC energy the range probed in x is somewhat limited (down to 10^{-3}), and the evolution might be only tested at the LHC. In this case the processes $g\mathcal{T} \rightarrow q\bar{q}X$ and $g\mathcal{T} \rightarrow ggX$ for dijet production should also be included in the calculation. At the level of formula (24), the expressions of [26] could be useful, but to proceed further in the derivation, one needs to compute an 8-point function (for the gg final state), which we leave for future work.

Finally, the final-state configuration studied in this paper requires both particles to be produced at forward rapidities, in order to avoid a large rapidity interval between them. The situation considered in [4] with one particle produced at forward rapidity and the other at mid-rapidity calls for the inclusion of other small- x QCD effects in the BFKL framework [19]. In the context of azimuthal angle correlations, these effects have been the focus of devoted studies [27, 28], however combining them with the CGC evolution included here is still an open and interesting problem.

Acknowledgments

I am grateful to Francois Gélis for providing his code that evolves the MV model with the BK equation. I also thank Raju Venugopalan for reading the manuscript and making valuable comments. This research was supported by RIKEN, Brookhaven National Laboratory and the U.S. Department of Energy [DE-AC02-98CH10886].

-
- [1] L.V. Gribov, E.M. Levin and M.G. Ryskin, *Phys. Rep.* **100** (1983) 1;
A.H. Mueller, *Parton saturation-an overview*, hep-ph/0111244;
E. Iancu and R. Venugopalan, *The color glass condensate and high energy scattering in QCD*, hep-ph/0303204;
H. Weigert, *Evolution at small $x(bj)$: the color glass condensate*, hep-ph/0501087.
- [2] P. Jacobs and X.N. Wang, *Prog. Part. Nucl. Phys.* **54** (2005) 443;
R. Baier, D. Schiff and B.G. Zakharov, *Ann. Rev. Nucl. Part. Sci.* **50** (2000) 37;
A. Kovner and U.A. Wiedemann, *Gluon radiation and parton energy loss*, hep-ph/0304151;
M. Gyulassy, I. Vitev, X.N. Wang and B.W. Zhang, *Jet quenching and radiative energy loss in dense nuclear matter*, nucl-th/0302077.
- [3] J. Casalderrey-Solana, E.V. Shuryak and D. Teaney, *Nucl. Phys.* **A774** (2006) 577.
- [4] D. Kharzeev, E. Levin and L. McLerran, *Nucl. Phys.* **A748** (2005) 627.
- [5] R. Baier, A. Kovner, M. Nardi and U.A. Wiedemann, *Phys. Rev.* **D72** (2005) 094013.

- [6] N.N. Nikolaev and W. Schäfer, *Phys. Rev.* **D71** (2005) 014023;
N.N. Nikolaev, W. Schäfer, B.G. Zakharov and V.R. Zoller, *Phys. Rev.* **D72** (2005) 034033.
- [7] I. Balitsky, *Nucl. Phys.* **B463** (1996) 99; *Phys. Lett.* **B518** (2001) 235;
Yu.V. Kovchegov, *Phys. Rev.* **D60** (1999) 034008; *Phys. Rev.* **D61** (2000) 074018.
- [8] L. McLerran and R. Venugopalan, *Phys. Rev.* **D49** (1994) 2233; *ibid.*, (1994) 3352; *Phys. Rev.* **D50** (1994) 2225;
A. Kovner, L. McLerran and H. Weigert, *Phys. Rev.* **D52** (1995) 6231; *ibid.*, (1995) 3809;
Y.V. Kovchegov, *Phys. Rev.* **D54** (1996) 5463; *Phys. Rev.* **D55** (1997) 5445;
R. Venugopalan, *Acta Phys. Polon.* **B30** (1999) 3731.
- [9] J. Jalilian-Marian, A. Kovner, A. Leonidov and H. Weigert, *Nucl. Phys.* **B504** (1997) 415; *Phys. Rev.* **D59** (1999) 014014;
J. Jalilian-Marian, A. Kovner and H. Weigert, *Phys. Rev.* **D59** (1999) 014015;
E. Iancu, A. Leonidov and L. McLerran, *Nucl. Phys.* **A692** (2001) 583; *Phys. Lett.* **B510** (2001) 133;
E. Ferreira, E. Iancu, A. Leonidov and L. McLerran, *Nucl. Phys.* **A703** (2002) 489;
H. Weigert, *Nucl. Phys.* **A703** (2002) 823.
- [10] C. Marquet, *Particle production and saturation at HERA*, hep-ph/0510176;
C. Marquet, *Mini review on saturation and recent developments*, hep-ph/0610300.
- [11] J. Jalilian-Marian and Y.V. Kovchegov, *Prog. Part. Nucl. Phys.* **56** (2006) 104.
- [12] F. Gélis and Y. Mehtar-Tani, *Phys. Rev.* **D73** (2006) 034019.
- [13] A. Kovner and U. Wiedemann, *Phys. Rev.* **D64**, (2001) 114002.
- [14] J. Jalilian-Marian and Y.V. Kovchegov, *Phys. Rev.* **D70** (2004) 114017; *Erratum-ibid.* **D71** (2005) 079901.
- [15] Yu.V. Kovchegov and A.H. Mueller, *Nucl. Phys.* **B529** (1998) 451;
A. Kovner and U. Wiedemann, *Phys. Rev.* **D64** (2001) 114002;
A. Dumitru and L. McLerran, *Nucl. Phys.* **A700** (2002) 492;
Yu. V. Kovchegov and K. Tuchin, *Phys. Rev.* **D65** (2002) 074026;
J.P. Blaizot, F. Gelis and R. Venugopalan, *Nucl. Phys.* **A743** (2004) 13;
C. Marquet, *Nucl. Phys.* **B705** (2005) 319; *Nucl. Phys.* **A755** (2005) 603c.
- [16] H. Fujii, F. Gelis and R. Venugopalan, *Nucl. Phys.* **A780** (2006) 146.
- [17] J.P. Blaizot, F. Gelis and R. Venugopalan, *Nucl. Phys.* **A743** (2004) 57.
- [18] K. Fukushima and Y. Hidaka, *Light projectile scattering off the Color Glass Condensate*, arXiv:0704.2806 [hep-ph].
- [19] L.N. Lipatov, *Sov. J. Nucl. Phys.* **23** (1976) 338;
E.A. Kuraev, L.N. Lipatov and V.S. Fadin, *Sov. Phys. JETP* **45** (1977) 199;
I.I. Balitsky and L.N. Lipatov, *Sov. J. Nucl. Phys.* **28** (1978) 822.
- [20] D.N. Triantafyllopoulos, *Nucl. Phys.* **B648** (2003) 293;
R. Peschanski and S. Sapeta, *Phys. Rev.* **D74** (2006) 114021;
R. Enberg, *Phys. Rev.* **D75** (2007) 014012;
G. Beuf and R. Peschanski, *Universality of QCD traveling waves with running coupling*, hep-ph/0702131.
- [21] C.S. Lam and G. Mahlon, *Phys. Rev.* **D61** (2000) 014005.
- [22] F. Gelis and A. Peshier, *Nucl. Phys.* **A697** (2002) 879.
- [23] S.S. Adler *et al.* [PHENIX Collaboration], *Phys. Rev. Lett.* **96** (2006) 222301;
J. Adams *et al.* [STAR Collaboration], *Phys. Rev. Lett.* **97** (2006) 152302.
- [24] I. Arsene *et al.* [BRAHMS Collaboration], *Nucl. Phys.* **A757** (2005) 1;
B.B. Back *et al.* [PHOBOS Collaboration], *Nucl. Phys.* **A757** (2005) 28;
J. Adams *et al.* [STAR Collaboration], *Nucl. Phys.* **A757** (2005) 102;
K. Adcox *et al.* [PHENIX Collaboration], *Nucl. Phys.* **A757** (2005) 184.
- [25] A. Dumitru, A. Hayashigaki and J. Jalilian-Marian, *Nucl. Phys.* **A765** (2006) 464.
- [26] N.N. Nikolaev, W. Schäfer and B.G. Zakharov, *Phys. Rev. Lett.* **95** (2005) 221803.
- [27] J. Bartels, V. Del Duca and M. Wusthoff, *Z. Phys.* **C76** (1997) 75;
A. Sabio Vera and F. Schwennsen, *Azimuthal decorrelation of forward jets in Deep Inelastic Scattering*, arXiv:0708.0549 [hep-ph].
- [28] V. Del Duca and C.R. Schmidt, *Nucl. Phys. Proc. Suppl.* **39BC** (1995) 137;
L.H. Orr and W.J. Stirling, *Phys. Rev.* **D56** (1997) 5875;
J. Kwiecinski, A.D. Martin, L. Motyka and J. Outhwaite, *Phys. Lett.* **B514** (2001) 355;
A. Sabio Vera, *Nucl. Phys.* **B746** (2006) 1;
A. Sabio Vera and F. Schwennsen, *The azimuthal decorrelation of jets widely separated in rapidity as a test of the BFKL kernel*, hep-ph/0702158;
C. Marquet and C. Royon, *Azimuthal decorrelation of Mueller-Navelet jets at the Tevatron and the LHC*, arXiv:0704.3409 [hep-ph].